Reply on CC1

Dear professor,

We sincerely thank you for your highly positive and constructive comments on our manuscript. We deeply appreciate your time and expertise, especially given your foundational contributions to coastal and intertidal remote sensing. Your insights regarding tidal biases and environmental scope are incredibly valuable and have significantly helped us improve the depth and rigor of our discussion. Below, we provide a point-by-point response to your comments. For your convenience, our direct responses are formatted in blue text, while the specific new content incorporated into the revised manuscript is highlighted in *blue italics*.

Comment 1:

The method relies heavily on the use of Sentinel-2 percentile composites to serve as machine learning covariates that reflectance tidal variability. However, due to persistent tidal biases associated with sun-synchronous sensors, satellites like Sentinel-2 rarely observes the same tidal conditions at different locations along the coastline (see Figure 8 in Bishop-Taylor et al. 2018 https://www.sciencedirect.com/science/article/pii/S0272771418308783, and Figure 7, Fitton et al. 2021 https://www.sciencedirect.com/science/article/pii/S2352938521000355). These biases mean that, for example, an 80th percentile composite in one location may observe high tide conditions, while the same 80th percentile composite in another location may only observe mid-tide. How does your approach handle these tide biases, and how do they affect the large-scale consistency of your results? There is currently a single sentence touching on tide variation issues in the manuscript ("First, regional variations in tidal regimes can alter the spectral-elevation relationship, affecting intertidal height retrieval") but I feel it needs to be elaborated on given the importance of these biases for large-scale coastal remote sensing analysis.

Reply 1：

We highly appreciate your insightful comment regarding the persistent tidal biases associated with sun-synchronous sensors. You have pointed out a fundamental and critical issue in large-scale coastal remote sensing, as comprehensively demonstrated in your work (Bishop-Taylor et al., 2019) and Fitton et al. (2021). We fully agree that if a sun-synchronous satellite repeatedly observes the same restricted phase of the tidal cycle, the physical meaning of the percentile composites will vary geographically, severely undermining large-scale consistency.

To rigorously address your concern and verify whether this tidal aliasing compromises our modeling in New Zealand, we conducted a systematic quantitative analysis using continuously measured tidal data. We downloaded the 1-minute interval sea-level records from 2018 to 2023 for 12 permanent tide gauge stations across New Zealand (provided by Land Information New Zealand, LINZ, http://sealevel-data.linz.govt.nz/tidegauge). For each station, we extracted the sea level at the exact Sentinel-2 overpass times and compared its statistical distribution with the natural, continuous full-tidal distribution.

The results strongly confirm that within the specific geographic and tidal context of New Zealand, the Sentinel-2 tidal bias is exceptionally minimal. As shown in Fig. 1 (using the Auckland and Napier station as an example) and summarized in Table 1, the 20th, 50th, and 80th percentiles derived solely from Sentinel-2 overpass moments are almost identical to the true tidal percentiles derived from the full 5-year continuous records.

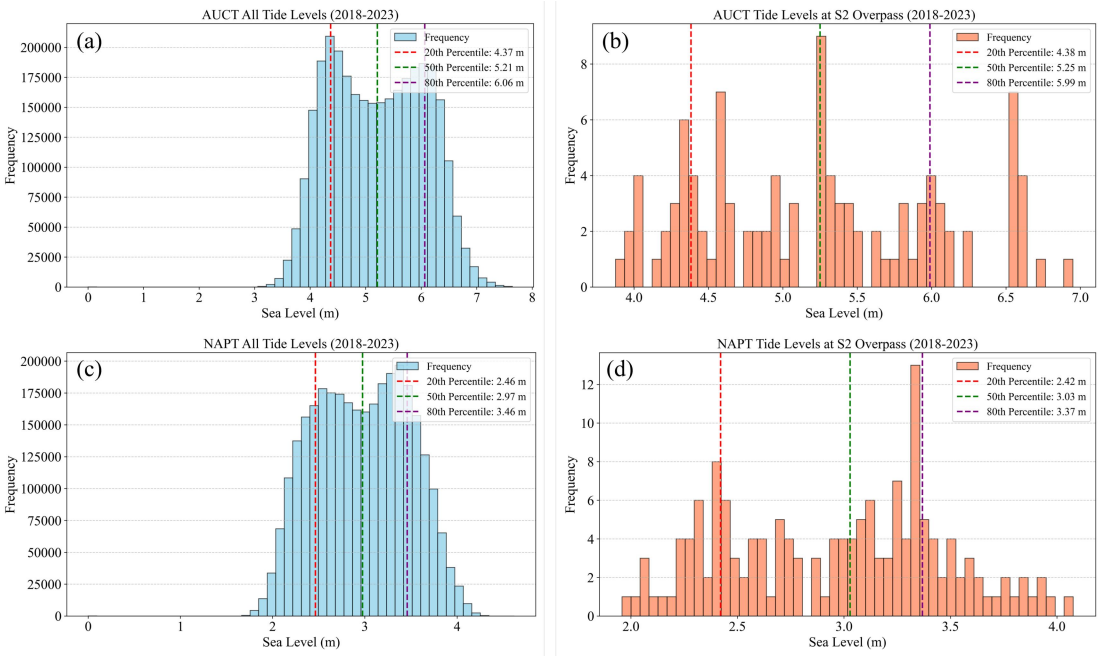

Fig. 1. Frequency histograms of tidal levels comparing continuous full-tidal records and Sentinel-2 (S2) overpass moments. Panels (a) and (b) represent the total observed tide level frequency histogram and the S2 observed tide level frequency histogram for the AUCT (Auckland) tide gauge station, respectively. Similarly, panels (c) and (d) display the total observed tide level frequency histogram and the S2 observed tide level frequency histogram for the NAPT (Napier) tide gauge station. The dashed vertical lines indicate the 20th, 50th, and 80th percentiles.

Table 1. The recorded values corresponding to the three percentiles (20th, 50th, and 80th) of the total continuous observations and the S2 overpass times across 12 representative tide gauge stations in New Zealand (2018–2023). This table also lists the geographic coordinates (longitude and latitude) where each station is located. The 12 analyzed stations are: AUCT (Auckland), CHIT (Chatham Islands), CPIT (Castlepoint), GBIT (Great Barrier Island), GIST (Gisborne), KAIT (Kaikoura), LOTT (Lottin Point), NAPT (Napier), OTAT (Port Chalmers), PUYT (Puysegur Point), TAUT (Tauranga), and WLGT (Wellington).

Station	Continuous tidal record (m)			Sentinel-2 overpass (m)			Lon (°)	Lat (°)
	20p	50p	80p	20p	50p	80p		
AUCT	4.37	5.21	6.06	4.38	5.25	5.99	174.79	-36.83

CHIT	2.22	2.57	2.96	2.21	2.50	2.82	-176.37	-44.02
CPIT	2.51	3.55	4.34	2.45	3.65	4.30	176.23	-40.90
GBIT	5.20	5.78	6.44	5.14	5.73	6.31	175.49	-36.19
GIST	3.41	3.88	4.37	3.50	3.83	4.31	178.02	-38.68
KAIT	1.49	2.00	2.54	1.40	1.89	2.49	173.70	-42.41
LOTT	2.99	3.54	4.06	3.02	3.59	4.12	178.16	-37.55
NAPT	2.46	2.97	3.46	2.42	3.03	3.37	176.92	-39.48
OTAT	3.83	4.39	5.00	3.83	4.29	4.78	170.63	-45.81
PUYT	5.78	6.37	6.96	5.79	6.29	6.78	166.59	-46.08
TAUT	4.37	4.94	5.47	4.41	4.98	5.49	176.18	-37.64
WLGT	2.52	2.88	3.29	2.53	2.86	3.21	174.78	-41.28

This remarkable consistency is primarily attributed to New Zealand's tidal regime, which is overwhelmingly dominated by the semi-diurnal lunar tide (M2) with a cycle of approximately 12.4 hours. Because the timing of high tide shifts by about 50 minutes each day, Sentinel-2's fixed ~22:00 UTC overpass naturally drifts through all phases of the tidal cycle over our 5-year observation window. Consequently, the satellite has successfully "sampled" the complete tidal range, ensuring that our 20th and 80th percentile spectral composites genuinely represent the physically wet (inundated) and dry (exposed) states across the national coastline.

Furthermore, to handle any minor residual regional tidal variations, our XGBoost model incorporates spatial and geometric features, including absolute geographic coordinates (X, Y) and relative distance metrics. As demonstrated by our SHAP analysis, this allows the machine learning framework to implicitly adapt to distinct regional spectral-elevation mappings and enforce a realistic topographic structure, rather than applying a rigid universal rule.

We recognize, however, exactly as you rightly pointed out, that this approach faces critical challenges when transferred to regions dominated by diurnal tides (where a

fixed overpass time may repeatedly capture the same restricted tidal phase). In such environments, tidal aliasing would severely distort the physical representation of the percentiles. We deeply appreciate your comment, which prompted us to explicitly define the environmental scope and limitations of our methodology.

We have significantly expanded the discussion on this tidal bias issue in Section 5.3 (Potential for global application and challenges). The revised text is as follows:

First, regional variations in tidal regimes can profoundly alter the spectral-elevation relationship, affecting intertidal height retrieval. Specifically, the persistent tidal biases associated with sun-synchronous sensors pose a major challenge for large-scale coastal remote sensing (Bishop-Taylor et al., 2019; Fitton et al., 2021). Our framework benefits from New Zealand's predominantly semi-diurnal tidal regime (M2 cycle of ~12.4 hours). Over the 5-year observation window, Sentinel-2's fixed overpass time naturally samples the complete range of tidal phases, ensuring that our multi-percentile composites genuinely reflect full tidal exposure dynamics. However, applying this statistical percentile approach to regions dominated by diurnal tides (where a fixed overpass time may repeatedly capture the same tidal phase, leading to severe tidal aliasing) will result in percentiles lacking consistent physical meaning. To mitigate this at a global scale, the temporal compositing strategy must be explicitly coupled with regional hydrodynamic models to strictly filter imagery based on absolute tidal stages rather than relying solely on observation percentiles. Additionally, implementing a regionalized modeling approach can further alleviate these spatial inconsistencies. By clustering coastal segments based on distinct tidal characteristics—such as tidal range, phase, and geomorphic type—independent, localized machine learning models can be trained to accurately capture the specific spectral-elevation relationships unique to each tidal zone.

Reference:

Bishop-Taylor, R., Sagar, S., Lymburner, L., and Beaman, R. J.: Between the tides: Modelling the elevation of Australia's exposed intertidal zone at continental scale,

Estuarine Coastal Shelf Sci., 223, 115-128, https://doi.org/10.1016/j.ecss.2019.03.006, 2019.

Fitton, J. M., Rennie, A. F., Hansom, J. D., and Muir, F. M. E.: Remotely sensed mapping of the intertidal zone: A Sentinel-2 and Google Earth Engine methodology, Remote Sens. Appl.: Soc. Environ., 22, 100499, https://doi.org/10.1016/j.rsase.2021.100499, 2021.

Comment 2:

The paper focuses primarily on open coast beach environments, which is a valuable niche for intertidal elevation modelling that has not seen as much research attention as more sheltered, tide dominated systems. However, I feel it would be valuable to also include either include an example of model performance across more extensive tidal flat environments, or include some discussion points about how/why these intertidal environments were excluded from the study.

Reply 2：

Thank you for this insightful suggestion. You have accurately captured the specific geomorphological niche of our study. We intentionally bounded our study domain to open sandy beaches (using the OpenStreetMap sandy beach polygons) and excluded extensive muddy tidal flats and estuarine systems.

This exclusion was driven by several physical and methodological considerations. Firstly, sandy beaches and muddy tidal flats exhibit fundamentally different spectral-elevation relationships. Extensive tidal flats typically possess much gentler gradients, distinct sediment properties (mud/silt vs. sand), and much higher moisture retention capacities due to more frequent and prolonged inundation. Training a single global model encompassing both environments without explicit geomorphological classification would dilute the model's accuracy and introduce cross-domain prediction errors.

Secondly, extending this topographic inversion method to extensive tidal flat

environments is highly feasible, but it requires further methodological refinement. Because tidal flats are wetter and often characterized by complex creek networks or transient biological cover (e.g., algal mats), accurate retrieval in these areas necessitates the introduction of additional spectral features. For instance, incorporating water and vegetation indices (such as the multi-percentile statistics of MNDWI and NDVI) is crucial for capturing the complex moisture dynamics. Furthermore, a regionalized modeling approach based on coastal typologies would be required to achieve high accuracy.

We fully agree that discussing this boundary is valuable for readers. We have added a dedicated paragraph in the Discussion section (Section 5.3) explaining the rationale for excluding extensive tidal flats and highlighting the distinct geomorphological and feature engineering considerations required for modeling those environments.

We have added the following paragraph to Section 5.3 (Potential for global application and challenges) to explicitly define our study boundary and discuss tidal flats:

Furthermore, it is important to note that the current framework is specifically optimized for and applied to open sandy beach environments, intentionally excluding extensive muddy tidal flats and estuarine systems. This boundary was established because sandy beaches and muddy tidal flats exhibit fundamentally different spectral-elevation relationships. Tidal flats typically possess much gentler gradients, distinct sediment properties (mud/silt), and higher moisture retention capacities due to more frequent and prolonged inundation. Consequently, applying this beach-focused model directly to tidal flats could introduce cross-domain prediction errors. Extending this topographic inversion method to extensive tidal flat environments is highly feasible but requires specific methodological refinements. Because tidal flats are significantly wetter, accurate retrieval would necessitate the introduction of additional feature variables, such as multi-percentile statistics of the Modified Normalized Difference Water Index (MNDWI) and Normalized Difference Vegetation Index (NDVI), to better capture complex moisture and biological dynamics. Additionally, implementing a regionalized modeling framework based on coastal geomorphological classification would be

essential to accurately map these distinct intertidal environments.

Comment 3:

The data package includes only data for the "NoData" voids in the DeltaDTM dataset. Are there plans to also provide a combined DeltaDTM + NZ-BeachTopo30 data as a single seamless topobathy DEM? Or is the expectation that downstream users will combine these datasets themselves?

Reply 3:

Thank you for carefully reviewing our data repository. We apologize for any confusion caused by our initial description on Zenodo. To clarify, the dataset currently provided in the data package is already the combined, seamless DEM (i.e., the original valid DeltaDTM backshore data completely mosaicked with our newly predicted intertidal topography). Downstream users do not need to perform any further integration themselves.

We realize that our previous Zenodo description stating "The model specifically targets and fills the 'NoData' voids in the DeltaDTM dataset" may have inadvertently implied that only the newly predicted pixels were included in the downloaded file. We highly appreciate you pointing this out.

To prevent any future misunderstandings, we have updated the Zenodo repository description to make it explicitly clear that the downloadable file (NZ-BeachTopo30) is the fully integrated, mosaicked beach topography DEM. Additionally, we have slightly refined the text in the "Data availability" (Section 6) of the revised manuscript to emphasize that the published dataset is a complete, mosaicked product.

Modifications in the revised manuscript (Section 6):

The final seamless beach topography dataset, NZ-BeachTopo30 (a fully integrated mosaicked product combining the DeltaDTM baseline and our newly predicted

intertidal elevations), is available on Zenodo via the digital object identifier (DOI): https://doi.org/10.5281/zenodo.17785546 (Wang, 2025).

Reply on RC1

General comments

I have reviewed the manuscript "NZ-BeachTopo30: Bridging the Intertidal Data Gap by Fusing ICESat-2 and Sentinel-2". Overall, this paper presents a novel and valuable dataset for New Zealand beach topography, filling an important data gap. The manuscript is generally well structured, and the methodology is clearly described. However, some revisions are still required to enhance the quality of the manuscript, and my specific comments are detailed as follows.

Reply: We sincerely thank you for your highly positive evaluation and constructive comments on our manuscript "NZ-BeachTopo30: A national-scale and full-coverage 30 m beach topography dataset for New Zealand reconstructed by fusing ICESat-2 and Sentinel-2". We deeply appreciate your recognition of the novelty and value of our dataset. Your detailed suggestions regarding the distinction of LiDAR systems, dataset URLs, explanation of spectral quantiles, the SMOGN algorithm, and the discussion on tidal flats are incredibly valuable. Incorporating your feedback has significantly enhanced the clarity, completeness, and rigor of our manuscript.

Below, we provide a point-by-point response to your comments. For your convenience, our direct responses are formatted in blue text, while the specific new content incorporated into the revised manuscript is highlighted in *blue italics*.

Comment 1:

In the introduction, the authors discuss the characteristics and limitations of airborne LiDAR and spaceborne LiDAR together. I recommend discussing them separately to better distinguish between the two in the manuscripts.

Reply 1:

Thank you for pointing out this important distinction. We fully agree that grouping airborne

and spaceborne LiDAR together obscures their distinct operational characteristics and limitations. Airborne LiDAR provides dense, continuous 3D point clouds but is often limited by high costs and regional coverage. In contrast, spaceborne LiDAR (such as ICESat-2) offers global coverage but only provides sparse, along-track elevation profiles rather than continuous wall-to-wall mapping.

To accurately reflect these differences, we have rewritten the corresponding paragraph in the Introduction to discuss them separately.

Modifications in the revised manuscript (Section 1, Introduction):

Airborne and spaceborne Lidar are widely regarded as the "gold standard" for elevation data, yet they possess distinct characteristics and limitations. Airborne laser scanning directly generates high-precision, dense three-dimensional point clouds that capture beach microtopography at centimeter-level resolution (Schmelz and Psuty, 2022; Stockdon et al., 2006). However, its application for rapid, country-wide beach monitoring is hindered by limited, strip-based coverage and high operational costs. Conversely, spaceborne Lidar (such as ICESat-2) offers unparalleled global coverage and frequent revisit cycles (Markus et al., 2017). While it provides highly accurate elevation control points, its measurements are confined to sparse, along-track profiles rather than spatially continuous surfaces (Markus et al., 2017), making it challenging to generate seamless wall-to-wall beach topography mapping independently.

Reference:

Markus, T., Neumann, T., Martino, A., Abdalati, W., Brunt, K., Csatho, B., Farrell, S., Fricker, H., Gardner, A., Harding, D., Jasinski, M., Kwok, R., Magruder, L., Lubin, D., Luthcke, S., Morison, J., Nelson, R., Neuenschwander, A., Palm, S., Popescu, S., Shum, C. K., Schutz, B. E., Smith, B., Yang, Y., and Zwally, J.: The Ice, Cloud, and land Elevation Satellite-2 (ICESat-2): Science requirements, concept, and implementation, Remote Sens. Environ., 190, 260-273, https://doi.org/10.1016/j.rse.2016.12.029, 2017.

Schmelz, W. J. and Psuty, N. P.: Application of geomorphological maps and LiDAR to volumetrically measure coastal geomorphological change from Hurricane Sandy at Fire

Island National Seashore, Geomorphology, 408, 108262, https://doi.org/10.1016/j.geomorph.2022.108262, 2022.

Stockdon, H. F., Holman, R. A., Howd, P. A., and Sallenger, A. H.: Empirical parameterization of setup, swash, and runup, Coastal Eng., 53, 573-588, https://doi.org/10.1016/j.coastaleng.2005.12.005, 2006.

Comment 2:

I suggest the authors ensure the completeness of information for all datasets used, as I noticed that some data sources do not have corresponding URLs provided. This is essential to guarantee data accessibility and the reproducibility of the methodology.

Reply 2:

We appreciate your meticulous review. We completely agree that providing data access links is essential for ensuring the transparency and reproducibility of the methodology. In the original manuscript, while the airborne Lidar link was provided, the URLs for other public datasets were inadvertently omitted. We have now systematically reviewed Section 2 and added the official data access URLs for DeltaDTM, Sentinel-2, ICESat-2, and OpenStreetMap (OSM) to the revised manuscript.

Modifications in the revised manuscript (Section 2):

We have added the following URLs to their respective subsections:

Section 2.2.1 (DeltaDTM): Added the data source link: "(available at https://doi.org/10.4121/21997565)".

Section 2.3.1 (Sentinel-2): Added the platform link: "The Sentinel-2 Level-2A products were accessed and processed via the Google Earth Engine (GEE) platform (https://earthengine.google.com)."

Section 2.3.2 (ICESat-2): Added the data source link: "This study employed the ATL03 Global Geolocated Photon data product (available at National Snow and Ice Data Center, NSIDC: _

https://nsidc.org/data/ATL03)."

Section 2.4 (Ancillary data): Added the OSM link: "...incorporated coastal geographic information from OpenStreetMap (OSM, https://osmdata.openstreetmap.de/)..."

Comment 3:

Sentinel-2 composite images serve as the foundation for beach topography modeling in this study. Hence, I recommend that the authors provide a more detailed explanation of the meaning of different quantiles derived from Sentinel-2 optical imagery.

Reply 3:

Thank you for this constructive recommendation. You are entirely correct that the percentile composites are the cornerstone of our modeling framework. We realize that the physical implication of these spectral quantiles needs to be articulated more explicitly, as the relationship between reflectance percentiles and tidal states can vary depending on local coastal environments and water turbidity.

To clarify this for the readers, we have expanded our explanation in Section 3.1.2. For the majority of open sandy beaches in New Zealand, where coastal waters are relatively clear, water and saturated sand tend to absorb solar radiation (resulting in lower reflectance), while exposed dry sand is highly reflective. Therefore, sorting the time-series observations into percentiles naturally stratifies the tidal conditions: the low-percentile composites (e.g., 20th percentile) typically capture the darker observations, which generally correspond to inundated or wetter states. Conversely, the high-percentile composites (e.g., 80th percentile) typically capture the brighter observations, generally corresponding to drier, exposed states. We have also added a nuance to acknowledge that while this relationship might be complicated in highly turbid waters, it holds as a robust general pattern for the open sandy beaches targeted in our study.

Modifications in the revised manuscript (Section 3.1.2):

This percentile compositing serves not only as a noise-filtering method but also embodies a physically meaningful grouping of tidal states. By aggregating multiple observations across the tidal cycle, the composite layers effectively capture the amplitude of reflectance variability caused by tidal inundation and moisture fluctuations. For most open sandy beaches characterized by relatively clear waters, water and saturated sand tend to absorb optical radiation (yielding lower reflectance), whereas exposed dry sand is typically highly reflective. Consequently, low-percentile composites (e.g., 20th percentile) typically isolate darker observations, which generally correspond to more frequently submerged or wetter states during high tides. Conversely, high-percentile composites (e.g., 80th percentile) tend to capture brighter observations, representing drier and more exposed states during low tides. While this reflectance-moisture relationship might be inverted or complicated in highly turbid coastal waters, it remains a robust general pattern for the open sandy beaches targeted in this framework. Feeding this consistent gradient of multi-percentile features allows the machine learning algorithm to implicitly deduce the topographic elevation gradient from the shoreline to the backshore.

Comment 4:

I suggest the authors supplement the paper with an explanation of the applicability of the SMOGN algorithm to regression tasks, or add relevant clarifications.

Reply 4:

Thank you for this valuable suggestion. It is indeed necessary to clarify this, as data-balancing techniques (like SMOTE) are widely known for classification tasks, but their application in continuous regression tasks is less commonly understood. SMOGN (Synthetic Minority Over-Sampling Technique for Regression with Gaussian Noise) is specifically tailored for imbalanced regression problems. We have added a brief explanation in Section 3.2.1 to clarify how SMOGN accommodates continuous elevation variables by utilizing a relevance function.

Modifications in the revised manuscript (Section 3.2.1):

Unlike traditional SMOTE, which is restricted to categorical classification tasks, SMOGN is specifically tailored for continuous regression problems. In topographic modeling, the target variable (elevation) is continuous. SMOGN addresses this by employing a user-defined relevance function to map the continuous elevation values into a bounded range [0, 1], identifying the rare extreme values (e.g., extreme low elevations in the subtidal zone) as the 'minority' cases. It then combines over-sampling and under-sampling strategies to generate synthetic samples...

Comment 5:

I suggest the authors also provide the latitude and longitude information for the beaches corresponding to panels a-f in Figure 5.

Reply 5:

Thank you for pointing out this omission. Providing the exact geographic coordinates will certainly help readers locate these specific validation beaches. We have updated Table 3 to include the central latitude and longitude for each of the six selected beaches (panels a-f in Figure 5).

Modifications in the revised manuscript (Table 3):

Table 1. Detailed information of the 6 randomly selected beaches for validation

Beach FID	***Geographic location (island)***	***Proportion of predicted pixels.***	***Longitude, Latitude (°)***
220	*South island*	*54.1%*	*171.626°E, 41.737°S*
222	*South island*	*75.9%*	*171.549°E, 41.749°S*
678	*South island*	*31.7%*	*170.199°E, 43.186°S*
343	*North island*	*35.2%*	*173.375°E, 34.931°S*

418	*North island*	*63.5%*	*177.304°E, 39.089°S*
421	*North island*	*39.6%*	*177.698°E, 39.053°S*

Comment 6:

It is suggested that the authors add relevant discussion and outlook in the discussion section regarding whether the proposed approach can be applied to the inversion of muddy tidal flat topography in the future.

Reply 6:

This is an excellent and forward-looking suggestion. Extending this topographic inversion method to extensive muddy tidal flat environments is highly feasible and represents the most important next step for our research. However, muddy tidal flats exhibit fundamentally different spectral-elevation relationships compared to sandy beaches, largely due to much gentler gradients, distinct sediment properties (mud/silt), and higher moisture retention capacities.

Following your suggestion, we have added a dedicated paragraph in the Discussion section (Section 5.3) to provide an outlook on how our proposed approach can be adapted for muddy tidal flat topography inversion in the future.

Modifications in the revised manuscript (Section 5.3):

Furthermore, while the current framework is specifically optimized for open sandy beaches, extending this topographic inversion approach to extensive muddy tidal flat environments is highly feasible and represents a critical future direction. Because tidal flats exhibit much gentler gradients, distinct sediment properties (mud/silt), and significantly higher moisture retention due to more frequent inundation, their spectral-elevation relationships differ fundamentally from those of sandy beaches. To successfully apply this approach to tidal flats, specific methodological refinements are required. Accurate retrieval in these wetter environments would necessitate the introduction of additional feature variables, such as

multi-percentile statistics of the Modified Normalized Difference Water Index (MNDWI) and Normalized Difference Vegetation Index (NDVI), to better capture complex moisture and transient biological dynamics (e.g., algal mats). Additionally, implementing a regionalized modeling framework based on coastal geomorphological classification would be essential to accurately map these distinct intertidal environments without introducing cross-domain prediction errors.

Reply on RC2

General comments

The study titled “NZ-BeachTopo30: A national-scale and full-coverage 30 m beach topography dataset for New Zealand reconstructed by fusing ICESat- 2 and Sentinel-2” presents a novel and robust methodology for generating topography for beaches and then develop a useful and national-scale dataset across New Zealand. Please find my revision suggestions below.

Reply: We sincerely thank you for your highly positive evaluation and constructive comments on our manuscript. We deeply appreciate your recognition of our methodology as "novel and robust" and the resulting dataset as a "useful and national-scale" contribution. Your detailed suggestions regarding the introduction’s logical flow, figure improvements (Figures 1, 2, and 14), quantitative explanation of percentile denoising, and the expansion of our discussion on limitations and potential applications are incredibly valuable. Incorporating your feedback has significantly enhanced the clarity, comprehensiveness, and readability of our manuscript.

Below, we provide a point-by-point response to your comments. For your convenience, our direct responses are formatted in blue text, while the specific new content incorporated into the revised manuscript is highlighted in *blue italics*.

Comment 1:

I suggest adding one sentence at the end of the second paragraph in the introduction to summarize the current status and limitations of remote sensing techniques for beach topography reconstruction. Moreover, the first sentence of the third paragraph in the introduction should be revised to provide a general overview of mainstream DEM datasets, so as to improve the logical coherence of the paragraph.

Reply 1:

Thank you for this excellent suggestion. We agree that adding a concluding summary to the second paragraph and a broader overview sentence to the beginning of the third paragraph greatly improves the logical transition and coherence of the Introduction. We have revised both paragraphs accordingly.

Modifications in the revised manuscript (Section 1, Introduction):

Added to the end of the second paragraph:

In summary, while current remote sensing techniques have significantly advanced coastal monitoring, achieving national-scale, high-resolution, and seamless beach topography reconstruction remains fundamentally constrained by the trade-offs between spatial coverage, temporal revisit frequency, and observation continuity.

Revised the second sentence of the third paragraph:

Currently, several mainstream global and regional DEM datasets, such as SRTM, Copernicus DEM, and AW3D30 (Farr et al., 2007; Takaku et al., 2016; Esa, 2024), are widely utilized for coastal studies; however, they often struggle to accurately capture the dynamic and frequently inundated intertidal zones, because they were primarily designed for inland areas.

Comment 2:

I suggest that ICESat-2 track information should be added in Figure 1 to better illustrate its spatial distribution across the study area.

Reply 2:

We completely agree with your suggestion. Visualizing the ICESat-2 ground tracks provides readers with a clear understanding of the spatial density and distribution of our training data across the study area. To ensure the original map remains clear and readable without becoming overcrowded, we have updated Figure 1 by adding a dedicated subpanel (panel b) that explicitly illustrates the spatial distribution of the ICESat-2 tracks across New Zealand. The figure caption has also been updated accordingly to reflect this addition.

Modifications in the revised manuscript:

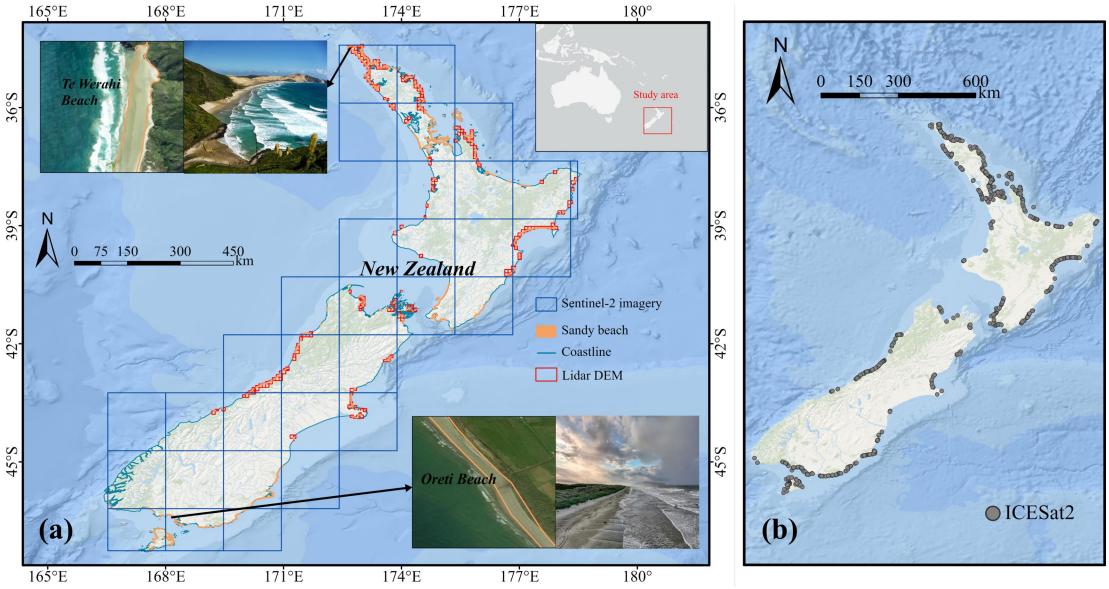

Fig. 1 Geographical information and dataset distribution across the study area (New Zealand). (a) The main map displays the spatial distribution of the study datasets: Sentinel-2 image footprints (n = 31; blue boxes), beach polygons (n = 1,713; orange), coastline (cyan lines), and Lidar DEM footprints (n = 309; red boxes). The inset panels, linked by arrows to their corresponding locations, illustrate two representative beaches selected from the North Island (Te Werahi Beach) and South Island (Oreti Beach). In each inset, the left subpanel displays high-resolution satellite imagery of the beach extent, while the right subpanel shows a corresponding field photograph. (b) The spatial distribution of the spaceborne ICESat-2 ground tracks utilized in this study. The background map for the main map and the high-resolution imagery for the insets are World Ocean Base and World Imagery, respectively, both served by Esri via ArcGIS Pro software.

Comment 3:

In Figure 2 workflow diagram, I suggest that the authors explicitly indicate that airborne LiDAR was used for validation; otherwise, it could easily be confused with the spaceborne ICESat-2 LiDAR data also employed in this study.

Reply 3:

Thank you for pointing out this potential source of confusion. We have updated the flowchart in Figure 2. The text block for airborne Lidar has been explicitly relabeled as "Airborne

LiDAR (Validation Data)" to clearly distinguish its role from the spaceborne ICESat-2 Lidar used for model training.

Modifications in the revised manuscript:

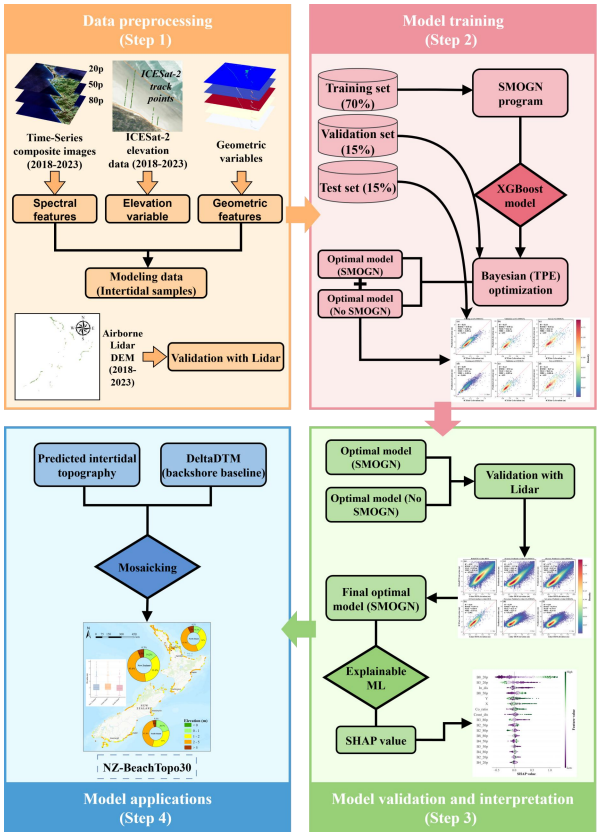

Fig. 2 Workflow used to reconstruct beach topography: (1) Data preprocessing (where 20p, 50p, and 80p refer to the 20th, 50th, and 80th percentile composite images, respectively); (2) Model training; (3) Model validation and interpretation; (4) Model applications.

Comment 4:

The authors used composite remote sensing imagery of different quantiles to represent states at various tidal levels and claimed that this method can achieve denoising effects. I recommend the authors provide more quantitative evidence to demonstrate the rationality of this approach used in this study.

Reply 4:

Thank you for your constructive comment. We understand that the use of multi-quantile composites requires robust justification both in terms of physical tidal representation and

statistical denoising effectiveness.

Firstly, regarding the physical rationality, we conducted a quantitative verification using 1-minute interval sea-level records from 12 permanent tide gauge stations across New Zealand (2018–2023). As shown in Fig. 3 (taking Auckland and Napier stations as examples) and Table 1 below, the tidal level distributions at Sentinel-2 overpass times perfectly align with the full continuous tidal cycle. The 20th, 50th, and 80th percentiles derived from satellite overpasses are nearly identical to the true natural tidal percentiles (with biases typically < 0.1 m). This proves that the 20th and 80th percentile spectral composites genuinely represent the physically wet/inundated and dry/exposed states, respectively.

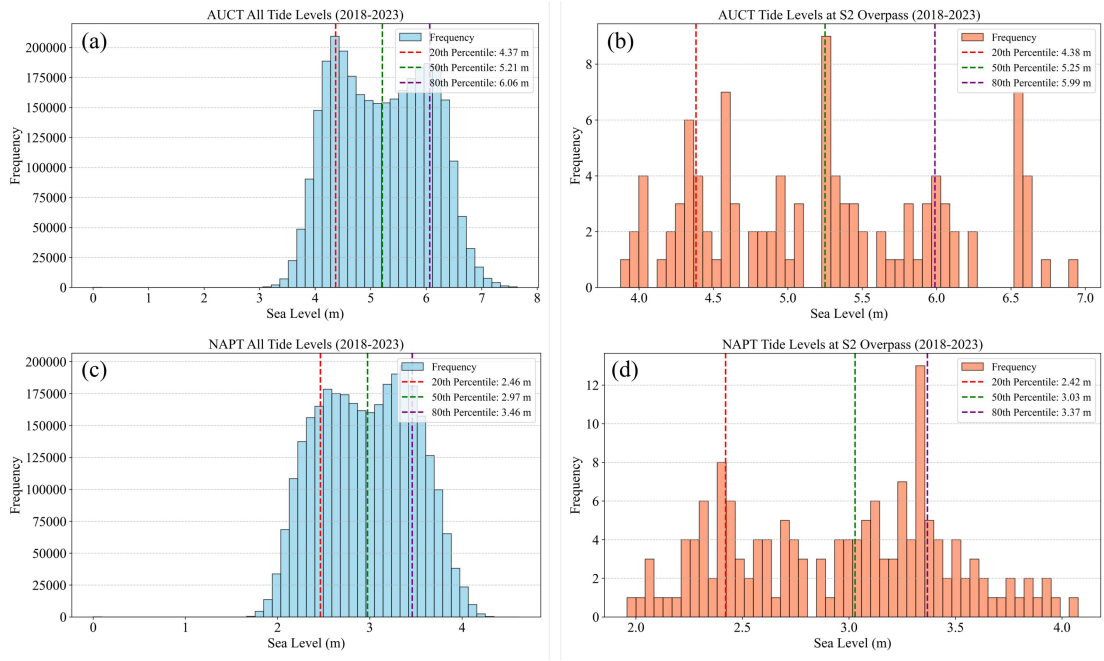

Fig. 3 Frequency histograms of tidal levels comparing continuous full-tidal records and Sentinel-2 (S2) overpass moments. Panels (a) and (b) represent the total observed tide level frequency histogram and the S2 observed tide level frequency histogram for the AUCT (Auckland) tide gauge station, respectively. Similarly, panels (c) and (d) display the total observed tide level frequency histogram and the S2 observed tide level frequency histogram for the NAPT (Napier) tide gauge station. The dashed vertical lines indicate the 20th, 50th, and 80th percentiles.

Table 1 The recorded values corresponding to the three percentiles (20th, 50th, and 80th) of the total continuous observations and the S2 overpass times across 12 representative tide

gauge stations in New Zealand (2018–2023). This table also lists the geographic coordinates (longitude and latitude) where each station is located. The 12 analyzed stations are: AUCT (Auckland), CHIT (Chatham Islands), CPIT (Castlepoint), GBIT (Great Barrier Island), GIST (Gisborne), KAIT (Kaikoura), LOTT (Lottin Point), NAPT (Napier), OTAT (Port Chalmers), PUYT (Puysegur Point), TAUT (Tauranga), and WLGT (Wellington).

Station	**Continuous tidal record (m)**			**Sentinel-2 overpass (m)**			**Lon (°)**	**Lat (°)**
	20p	50p	80p	20p	50p	80p		
AUCT	4.37	5.21	6.06	4.38	5.25	5.99	174.79	-36.83
CHIT	2.22	2.57	2.96	2.21	2.50	2.82	-176.37	-44.02
CPIT	2.51	3.55	4.34	2.45	3.65	4.30	176.23	-40.90
GBIT	5.20	5.78	6.44	5.14	5.73	6.31	175.49	-36.19
GIST	3.41	3.88	4.37	3.50	3.83	4.31	178.02	-38.68
KAIT	1.49	2.00	2.54	1.40	1.89	2.49	173.70	-42.41
LOTT	2.99	3.54	4.06	3.02	3.59	4.12	178.16	-37.55
NAPT	2.46	2.97	3.46	2.42	3.03	3.37	176.92	-39.48
OTAT	3.83	4.39	5.00	3.83	4.29	4.78	170.63	-45.81
PUYT	5.78	6.37	6.96	5.79	6.29	6.78	166.59	-46.08
TAUT	4.37	4.94	5.47	4.41	4.98	5.49	176.18	-37.64
WLGT	2.52	2.88	3.29	2.53	2.86	3.21	174.78	-41.28

Secondly, regarding the denoising effect, the choice of intermediate percentiles (e.g., 20th and 80th) instead of absolute extrema (0th or 100th) is a widely recognized statistical strategy in coastal remote sensing to exclude episodic outliers (Bishop-Taylor et al., 2019; Zhao et al., 2020). In long-term time-series optical data, the 0–10th percentiles are frequently contaminated by residual cloud shadows or sensor anomalies (extreme low-reflectance noise), while the 90–100th percentiles often capture transient sunglint, whitecaps, or missed cloud pixels (extreme high-reflectance noise). By trimming the extreme 20% at both ends of the distribution, our method quantitatively suppresses these transient noises while robustly retaining the stable spectral signals of the tide-affected beach surface.

To transparently address your comment in the text, we have added a new paragraph in Section 3.1.2 of the revised manuscript to explicitly explain this denoising rationale. Additionally, we have compiled the quantitative validation results of the tide gauge stations into a newly created Supplementary Material file.

Modifications in the revised manuscript (Section 3.1.2):

This percentile compositing serves as both a physically meaningful stratification and a robust statistical denoising mechanism. Quantitative validation using 12 tide gauge stations across New Zealand confirms that the 20th, 50th, and 80th percentiles of Sentinel-2 overpass tidal levels closely match the full natural tidal range (biases < 0.1 m; see Fig. S1 and Table S1 in the Supplementary Material). From a statistical perspective, extracting specific intermediate quantiles rather than absolute extrema (0th or 100th percentiles) is a widely recognized method for effectively filtering out episodic noise in time-series satellite imagery (Bishop-Taylor et al., 2019; Zhao et al., 2020). Specifically, trimming the extreme tails of the distribution removes residual cloud shadows (low-reflectance outliers) and sunglint or whitecaps (high-reflectance outliers), thereby ensuring that the machine learning model is trained on stable, tide-representative spectral features.

Reference:

Bishop-Taylor, R., Sagar, S., Lymburner, L., and Beaman, R. J.: Between the tides: Modelling the elevation of Australia's exposed intertidal zone at continental scale, Estuarine Coastal Shelf Sci., 223, 115-128, https://doi.org/10.1016/j.ecss.2019.03.006, 2019.

Zhao, C., Qin, C.-Z., and Teng, J.: Mapping large-area tidal flats without the dependence on tidal elevations: A case study of Southern China, ISPRS J. Photogramm. Remote Sens., 159, 256-270, https://doi.org/10.1016/j.isprsjprs.2019.11.022, 2020.

Comment 5:

I suggest the authors add boxplots for the X-axis and Y-axis corresponding data in panels a and b of Figure 14 in Section 5.2, to enable a more intuitive comparison. In addition, In Figure 14, it is evident that DeltaDTM systematically omits low-lying areas of beaches as

well as regions adjacent to the ocean. I suggest that the authors emphasize this point in their discussion.

Reply 5:

We greatly appreciate these insightful suggestions.

First, we have updated Figure 14 by adding marginal boxplots to both the X and Y axes in panels (a) and (b). As you rightly anticipated, these boxplots make the density and distribution comparisons much more intuitive.

Second, your observation regarding DeltaDTM's systematic omission is remarkably acute and is now perfectly visualized by the newly added boxplots. In panel (b), the Y-axis boxplot (representing DeltaDTM inundated areas) is heavily compressed near zero, whereas the corresponding X-axis Lidar boxplot shows a wide distribution of actual inundation. This quantitatively confirms that DeltaDTM systematically assigns 'NoData' or positively biased elevations to low-lying beaches and regions immediately adjacent to the ocean, preventing accurate simulated inundation.

We have explicitly emphasized this critical point in the Discussion (Section 5.2) to highlight the value of our newly generated dataset in bridging these specific nearshore data gaps, and updated the caption for Figure 14 accordingly.

Modifications in the revised manuscript (Section 5.2):

As intuitively demonstrated by the scatter distributions and the newly added marginal boxplots in Figure 14, it is evident that the baseline DeltaDTM systematically omits low-lying beach areas and regions immediately adjacent to the ocean (often returning 'NoData' or severely positively biased elevations). This systematic omission highlights the limitations of traditional global DEMs in capturing the intertidal zone. In contrast, our proposed framework successfully reconstructs these missing nearshore gradients, effectively bridging the critical data gap between the ocean and the backshore.

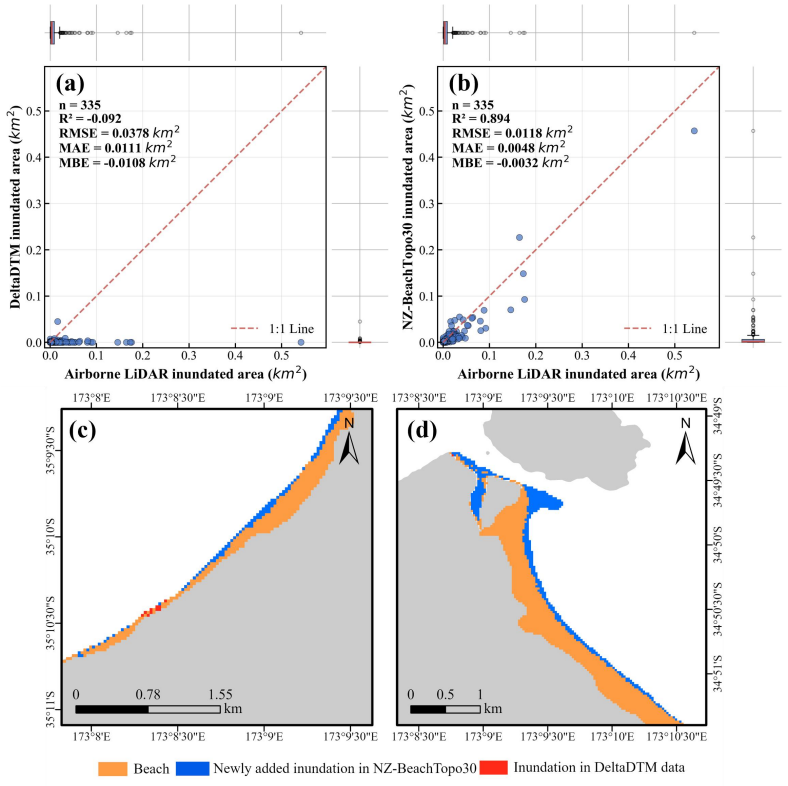

Fig. 4 Comparison of estimated inundation area and spatial patterns under a 1 m sea-level rise scenario. (a) Scatter plot and marginal boxplots of inundation area derived from the NZ-BeachTopo30 dataset versus the Lidar DEM reference. (b) Scatter plot and marginal boxplots of inundation area derived from the baseline DeltaDTM versus the Lidar DEM reference. The marginal boxplots intuitively illustrate the data distribution along the corresponding axes. (c) and (d) Spatial inundation patterns for two representative beach units. Orange areas indicate the beach extent, red areas indicate inundation simulated by the original DeltaDTM (inundation in DeltaDTM data), and blue areas indicate additional inundation identified by NZ-BeachTopo30 (newly added inundation in NZ-BeachTopo30). The land masks used as the background in panels (c) and (d) are from OSM.

Comment 6:

I suggest that the authors add a discussion in this section addressing potential limitations of this study. For example, the use of OSM data to delineate beach extents may introduce errors inherent to the baseline data itself. Beaches undergo long-term evolution, and their temporal changes are also critical. Additionally, the 10 m spatial resolution may be insufficient for

accurately representing narrower beaches. In summary, I would like to see the authors expand the discussion to include these considerations in the manuscript.

Reply 6:

We sincerely thank you for highlighting these important aspects. Discussing these limitations provides a much more comprehensive and objective perspective for the readers. We have added a dedicated paragraph addressing the inherent OSM baseline errors, the masking of temporal morphodynamics due to our 5-year time-series compositing, and the spatial resolution constraints (please note that our dataset has a spatial resolution of 30 m, aligning with the Sentinel-2 feature integration and DeltaDTM baseline, which, as you correctly pointed out, may still be insufficient for extremely narrow beaches).

Modifications in the revised manuscript (Section 5.3):

While our framework successfully generates national-scale beach topography, several limitations must be acknowledged. First, the spatial extent of the modeled beaches is inherently constrained by the baseline OpenStreetMap (OSM) polygons. Consequently, any existing omissions or geometric inaccuracies within the crowdsourced OSM data may propagate into our final maps. Second, our dataset represents a temporally composited 'mean state' generated from a 5-year observation window (2018–2023). Because sandy beaches are highly dynamic environments undergoing continuous morphological evolution (erosion and accretion), this static dataset cannot capture short-term temporal changes or extreme storm-induced morphodynamics. Finally, while the 30 m spatial resolution of the NZ-BeachTopo30 dataset is highly suitable for national- and regional-scale assessments, it may be insufficient for accurately resolving the micro-topography of extremely narrow or pocket beaches, where higher-resolution imagery would be required.

Comment 7:

This study presents a useful and large-scale dataset that fills an important gap in coastal elevation data for New Zealand. Hence, I suggest that the authors provide a more systematic

explanation regarding the advantages, significance, and potential application scenarios of the data.

Reply 7:

Thank you for this encouraging comment. To better underscore the value of the NZ-BeachTopo30 dataset, we have expanded the conclusion section to systematically outline its advantages and explicitly list its potential application scenarios for downstream users.

Modifications in the revised manuscript (Section 7, Conclusion):

In conclusion, the NZ-BeachTopo30 dataset fills a critical coastal elevation data gap by providing a seamless, high-accuracy, and spatially continuous 30 m topographic product for New Zealand's sandy beaches. Its primary advantage lies in overcoming the systematic omissions of low-lying intertidal zones typical of existing global DEMs. This dataset holds significant potential for a wide range of downstream applications. It provides essential baseline data for precise coastal hydrodynamic modeling (e.g., wave run-up and inundation models), regional vulnerability and risk assessments under future sea-level rise scenarios, and the strategic planning of coastal engineering and ecological conservation efforts.

Reply on RC3

General comments

This manuscript by Wang et al. presents NZ-BeachTopo30, a 30 m beach topography dataset for New Zealand that fills intertidal data voids in DeltaDTM by fusing ICESat-2 photon-counting altimetry with Sentinel-2 multispectral composites via XGBoost. The problem is well-motivated — intertidal voids in global coastal DEMs are a genuine and widely recognised obstacle for coastal hazard assessment — and the dataset itself is a welcome contribution. The production workflow is clearly described, the validation framework is multi-layered, and the sea-level rise demonstration nicely illustrates the practical value of improved intertidal coverage. I have only a few minor comments.

Reply:

We sincerely thank the reviewer for the thoughtful and constructive comments on our manuscript. We appreciate the recognition that the problem is well motivated, the dataset is a welcome contribution, and the production workflow and validation framework are clearly described. The reviewer's suggestions about framing the novelty more precisely around the data product and fusion design, clarifying the transferability assessment, emphasizing the intertidal validation metrics, discussing the Lidar resampling effect, refining the SHAP interpretation, and providing details on the vertical datum conversion are all highly valuable. Incorporating these comments has improved the clarity, accuracy, and completeness of our manuscript.

Below, we provide a point-by-point response to your comments. For your convenience, our direct responses are formatted in blue text, while the specific new content incorporated into the revised manuscript is highlighted in *blue italics*.

Comment 1:

The manuscript positions NZ-BeachTopo30 as "the first spatially continuous and full-

coverage beach topography dataset for New Zealand." The national-scale application and the specific integration strategy with DeltaDTM are clearly valuable. That said, the ICESat-2 + Sentinel-2 + ML approach for coastal elevation estimation has been demonstrated in several publications, and XGBoost for structured regression is well established. The authors might consider framing the novelty more precisely around the data product and the fusion design rather than the methodology itself — this would make the contribution stand out more clearly on its own merits.

Reply 1:

We thank the reviewer for this constructive suggestion. We agree that the methodological components (ICESat-2, Sentinel-2, and XGBoost) have been individually applied in previous coastal studies. Therefore, we have revised the manuscript to reframe the contribution more clearly around the data product itself and the specific fusion design that combines a high-accuracy baseline (DeltaDTM) with machine-learning-predicted intertidal elevations to achieve seamless spatial continuity.

Specifically, we have made the following modifications:

1. In the abstract, we have refined the wording to emphasize the data product and the fusion design. The revised text now states that the dataset is constructed by fusing ICESat-2 and Sentinel-2 within a framework that uses DeltaDTM as the backshore baseline, and that the key contribution is a national-scale dataset that bridges the intertidal data gap.

2. In the introduction (Section 1), we have revised the sentence that previously claimed the first spatially continuous dataset to more precisely highlight that the full-coverage reconstruction is achieved by the specific fusion design. The revised text now reads: Unlike existing global DEMs that contain systematic voids in intertidal zones, NZ-BeachTopo30 provides seamless spatial continuity from backshore to foreshore by integrating a high-accuracy baseline (DeltaDTM) with machine-learning-predicted elevations for previously missing intertidal areas. To our knowledge, this dataset represents the first national-scale product that achieves such complete topographic coverage for New Zealand’s sandy beaches through this targeted fusion strategy.

3. In the conclusion (Section 7), we have added a sentence that states the contribution in terms of the data product and fusion framework without using negative phrasing. The revised text now reads: NZ-BeachTopo30 is the first national-scale beach topography dataset for New Zealand that achieves full spatial coverage from backshore to foreshore. This is enabled by a fusion framework that combines a high-accuracy backshore baseline (DeltaDTM) with machine-learning-based intertidal elevation reconstruction using ICESat-2 and Sentinel-2 data. The resulting product provides seamless topographic continuity across the land-sea interface and fills a critical data gap for coastal applications in New Zealand.

These revisions ensure that the contribution is framed around the data product and the integration strategy, which are the genuine merits of this work.

Modifications in the revised manuscript:

Abstract (modified text):

Using DeltaDTM as a high-precision baseline for the stable backshore, we trained an XGBoost model on ICESat-2 control points and Sentinel-2 spectral-geometric features to reconstruct the missing intertidal topography specifically.

Introduction (Section 1, revised sentence):

To our knowledge, NZ-BeachTopo30 represents the first spatially continuous and high-resolution national-scale beach topography dataset for New Zealand. Unlike existing global DEMs that contain systematic voids in intertidal zones, NZ-BeachTopo30 provides seamless spatial continuity from backshore to foreshore by integrating a high-accuracy baseline (DeltaDTM) with machine-learning-predicted elevations for previously missing intertidal areas. It provides a full-coverage description of the beach surface and offers a new foundation for further applications.

Conclusion (Section 7, added sentence):

NZ-BeachTopo30 is the first national-scale beach topography dataset for New Zealand that achieves full spatial coverage from backshore to foreshore. This is enabled by a fusion framework that combines a high-accuracy backshore baseline (DeltaDTM) with machine-

learning-based intertidal elevation reconstruction using ICESat-2 and Sentinel-2 data. The resulting product provides seamless topographic continuity across the land-sea interface and fills a critical data gap for coastal applications in New Zealand.

Comment 2:

The 4,392 valid ICESat-2 pixels span 340 of 1,576 beach units (~22%). The transferability analysis in Section 4.4 is a real strength of the paper, and the modest degradation in accuracy (RMSE 0.93 → 1.02 m) is reassuring. It may be worth noting that this assessment can only be carried out where airborne Lidar is available, which itself tends to be concentrated in more accessible or higher-priority coastal segments. A brief acknowledgement of whether performance on remote, unsampled beaches might differ would give readers a more complete picture.

Reply 2:

We thank the reviewer for this thoughtful observation. We agree that the transferability analysis, while a strength of the paper, is necessarily constrained by the availability of airborne Lidar validation data. The reviewer correctly notes that Lidar coverage tends to be concentrated in more accessible or higher-priority coastal segments, and performance on remote, unsampled beaches could differ from the reported metrics. We have therefore added a brief acknowledgement of this limitation in the discussion section to provide readers with a more complete picture of the dataset's expected performance across different beach types.

Specifically, we have added a new paragraph in Section 5 (Discussion) that addresses this point. The added text acknowledges that the validation beaches with Lidar coverage may not be fully representative of all beach environments in New Zealand, and that caution is warranted when extrapolating the reported accuracy to remote or poorly sampled beaches. We also note that the transferability analysis in Section 4.4 already shows a modest degradation in accuracy from beaches with ICESat-2 training samples (RMSE = 0.93 m) to those without (RMSE = 1.02 m), which provides some indication of the model's robustness. However, we explicitly state that without independent validation data for those remote beaches, the exact performance remains uncertain.

Modifications in the revised manuscript (Section 5, added paragraph):

One limitation of the transferability analysis presented in Section 4.4 is that the validation using airborne Lidar is only possible where such data are available. In New Zealand, airborne Lidar coverage is not uniformly distributed across all coastal segments; it is more frequently available in accessible areas or those with higher priority for coastal management. Consequently, the reported accuracy metrics for beaches without ICESat-2 training samples (mean RMSE = 1.02 m) are derived from a set of validation beaches that may not fully represent the diversity of all unsampled beach environments across the country. The performance of the model on remote, poorly accessible, or low-priority beaches could differ from these reported values. While the modest degradation in accuracy from 0.93 m to 1.02 m (Section 4.4) suggests that the model generalizes reasonably well to beaches without direct training data, the absence of independent high-precision validation for those specific locations means that the exact accuracy remains unknown. Users of the NZ-BeachTopo30 dataset should be aware of this limitation when applying the product to remote or unsampled coastal segments.

Comment 3:

The internal model evaluation (Fig. 3) against ICESat-2 train/val/test splits usefully demonstrates model consistency, while the independent Lidar comparison (Fig. 4) provides the more informative accuracy diagnostic. It might be worth giving slightly more prominence to Fig. 4(f) — the accuracy specifically within the newly predicted intertidal voids (R^2 = 0.61, RMSE = 0.94 m) — since this is the metric most directly relevant to the paper's core contribution. The combined-product metrics (R^2 = 0.75, RMSE = 1.17 m) include the high-quality DeltaDTM backshore pixels and could, on their own, give readers a somewhat optimistic impression of the ML prediction component. Relatedly, the Lidar DEM was resampled from 1 m to 30 m via mean aggregation; on steeper beach faces this could introduce representativeness differences that inflate apparent disagreement. A brief note on this point would be helpful.

Reply 3:

We thank the reviewer for these constructive suggestions. We agree that Figure 4(f), which shows the accuracy specifically within the newly predicted intertidal voids ($R^2 = 0.61$, RMSE = 0.94 m), is the metric most directly relevant to the core contribution of the paper. We also agree that the combined product metrics ($R^2 = 0.75$, RMSE = 1.17 m) include the high quality DeltaDTM backshore pixels and could, if considered alone, give readers an overly optimistic impression of the machine learning prediction component. Furthermore, the reviewer raises an important point about the Lidar resampling procedure. The mean aggregation from 1 m to 30 m could indeed introduce representativeness differences on steeper beach faces, where elevation varies more rapidly across space, potentially inflating the apparent disagreement between the predicted and reference elevations.

We have therefore made the following modifications to address these points:

1. To give more prominence to Figure 4(f), we have revised the text in Section 4.2 (Accuracy assessment using Lidar DEM) to explicitly state that this metric is the most direct indicator of the model's performance in the intertidal zones that were originally missing from DeltaDTM. We have also added a cautionary note that the combined product metrics should be interpreted with the understanding that they benefit from the inclusion of the high accuracy DeltaDTM backshore pixels.

2. Regarding the Lidar resampling issue, we have added a brief note in Section 3.1.1 (Public topographic data preprocessing) where the resampling procedure is described. The added sentence acknowledges that mean aggregation on steep beach faces may smooth local topographic variations and introduce representativeness differences, which could contribute to the observed error metrics.

Modifications in the revised manuscript:

Section 4.2 (modified text, added sentences after presenting Figure 4(f)):

Among these validation results, the accuracy within the newly predicted intertidal voids (Figure 4(f); $R^2 = 0.61$, RMSE = 0.94 m, MAE = 0.70 m) directly indicates the model's ability to reconstruct the topography originally missing from the DeltaDTM baseline. This sub-meter accuracy demonstrates the effectiveness of the gap filling approach. The combined product

metrics for the entire study area (Figure 4(e); $R^2 = 0.75$, RMSE = 1.17 m, MAE = 0.82 m) include the high quality DeltaDTM backshore pixels and therefore reflect the performance of the integrated product, not solely the machine learning prediction component.

Section 3.1.1 (modified text, added sentence after describing the mean aggregation resampling):

It should be noted that on steeper beach faces, where elevation varies rapidly across short distances, this mean aggregation may smooth local topographic variations and introduce representativeness differences between the original 1 m resolution data and the resampled 30 m pixels. Such differences could contribute to the observed disagreement between the predicted elevations and the Lidar reference, particularly in areas with sharp elevation gradients.

Comment 4:

The SHAP analysis is well executed and adds useful transparency to the modelling. The main findings — NIR reflectance correlating positively with elevation, distance-to-coast tracking the cross-shore gradient — align with established coastal remote sensing understanding. The analysis is valuable precisely as confirmation that the model has learned physically sensible relationships. The authors might consider framing it in those terms rather than as a discovery of "physical driving mechanisms," which could slightly overstate what the interpretability exercise reveals.

Reply 4:

We thank the reviewer for this positive and constructive comment. We agree that the SHAP analysis primarily serves to confirm that the model has learned physically sensible relationships, rather than to discover new physical driving mechanisms. The reviewer correctly notes that the main findings, such as the positive correlation between NIR reflectance and elevation and the role of distance to coastline in tracking the cross-shore gradient, align with established coastal remote sensing understanding. Therefore, we have revised the manuscript to reframe the interpretation of the SHAP analysis in more accurate terms, avoiding overstatement of what the interpretability exercise reveals.

Specifically, we have made the following modifications in Section 4.5:

We revised the opening sentence of the first paragraph to state that the visualizations help examine how the model uses input features, rather than interpreting the model from different perspectives in a way that might imply discovery of new mechanisms.

We revised several sentences throughout the section that previously used phrases such as indicates that the model effectively leverages the physical principle, confirms the dominant mechanisms driving the intertidal reconstruction, and clarifies how the model resolves the intertidal interface. These have been replaced with more neutral phrasing that emphasizes confirmation of expected physical relationships rather than discovery.

We revised the final sentence of the section to avoid claiming that the model captures regional-scale variations as a novel finding, instead stating that the patterns align with expectations.

Modifications in the revised manuscript (Section 4.5, full revised text):

Based on the computed SHAP values, three types of visualizations were generated to examine how the model uses input features for elevation prediction. The first is the SHAP summary plot, which conveys feature importance and the direction of impact. Features are ranked in descending order of global significance, represented by their mean absolute SHAP values. Each point in the plot corresponds to a single sample; the color indicates the magnitude of the feature value, while the horizontal position denotes the direction (positive or negative) and strength of its contribution to the prediction. The second visualization is the SHAP feature-interaction heatmap, which illustrates the average interaction intensity between pairs of important features. Finally, the SHAP dependence plot was used to investigate the effects of individual features further. For the six most important features identified in the summary plot, dependence graphs were generated to show the relationship between each feature's actual value and its corresponding SHAP value.

High near-infrared (NIR) reflectance is associated with higher predicted beach elevation (Fig. 12(a)). Among all predictors, B8_20p (the 20th percentile of the near-infrared band) contributes most positively to the model output. This is consistent with the physical principle

of strong water absorption in the NIR spectrum, where high NIR values correspond to dry, exposed supratidal sands and low NIR values are characteristic of frequently inundated intertidal zones. Conversely, B3_20p (the 20th percentile of the green band) has the strongest negative effect. High green band reflectance is typically associated with shallow water bodies or moist sediments in low lying areas, which the model correctly interprets as indicators of lower elevation. Geometric and positional features such as In_dis, Coast_dis, Co_ratio, X, and Y also rank among the most influential variables, indicating that the model uses spatial context to enforce a realistic topographic structure where predicted elevations follow a plausible cross-shore geomorphological gradient.

The distribution of SHAP values across all samples (Fig. 12(b)) shows that B8_20p has a clear positive contribution trend, while B3_20p exhibits variable and opposing effects. This confirms that the model relies heavily on the moisture sensitive NIR band to resolve the primary elevation gradient from the sea to the land. Spatial and geometric features consistently show positive SHAP values, reinforcing their supportive role in refining the spatial continuity of the beach profile. The variability in SHAP values arises from the heterogeneity of coastal conditions, reflecting that the model captures distinct spectral-topographic relationships across the backshore, foreshore, and intertidal zones.

Nonlinear feature responses (Fig. 12(c)) further illustrate how the model handles the intertidal interface. B8_20p exhibits a sharp monotonic increase in SHAP values at lower reflectance ranges before stabilizing at high levels. This steep rising segment corresponds to the transition from the wet intertidal zone to the dry backshore, demonstrating that the model is sensitive to moisture changes in this critical zone. In contrast, B3_20p displays a pronounced negative trend that levels off at moderate reflectance, consistent with its association with low lying wet areas or shallow water. In_dis shows a nonlinear response with substantial variability, reflecting the complex morphological transition between landward and seaward beach zones. B8_50p follows a positive trend similar to B8_20p but with earlier saturation, suggesting that using multi-percentile statistics allows the model to capture temporal variations in tidal exposure. Geographic coordinates (X, Y) reveal broad spatial gradients in predicted elevation that are further modulated by spectral variables,

indicating regional scale variations in coastal morphology. These findings align with established coastal remote sensing understanding and confirm that the model's predictions are based on interpretable, physically meaningful features.

Comment 5:

Finally, the conversion from NZVD2016 to EGM2008 orthometric heights (lines 188–190) is an important step but is described only briefly. The difference between these two vertical reference surfaces varies spatially across New Zealand. It would be helpful if the authors could indicate the approximate magnitude and spatial pattern of this offset, so that readers can judge whether residual datum inconsistencies contribute meaningfully to the reported error budget.

Reply 5:

We thank the reviewer for raising this important technical point. The conversion from NZVD2016 to EGM2008 orthometric heights is indeed a critical step for ensuring vertical consistency across datasets. The reviewer correctly notes that the difference between these two vertical reference surfaces varies spatially across New Zealand, and understanding this variation is essential for interpreting the reported error budget.

To address this comment, we performed a quantitative analysis of the offset between NZVD2016 and EGM2008 across New Zealand. Specifically, we computed the difference between the EGM2008 geoid height and the NZGeoid2016 quasigeoid height ($N_{EGM2008}-N$) on a common grid. The resulting spatial pattern is shown in Fig. 1 (which will be included as Fig. S2 in the Supplementary Material of the revised manuscript). As illustrated in the figure, the offset ranges from approximately -1.365 m to +0.015 m across the country. The largest negative offsets (down to -1.365 m) occur in the South Island mountainous regions, where the EGM2008 geoid is substantially lower than the NZGeoid2016 quasigeoid. In coastal and beach areas, which are the primary focus of this study, the offset values are consistently close to zero, with a maximum of 0.015 m.

We have added the following information to the revised manuscript in Section 3.1.1, and we have prepared a new supplementary figure (Fig. S2) showing the offset map, which is

reproduced below as Fig. 1 in this reply. Importantly, the added text in Section 3.1.1 only describes the spatial pattern of the offset and refers readers to the supplementary figure, without introducing results or making claims about the error budget.

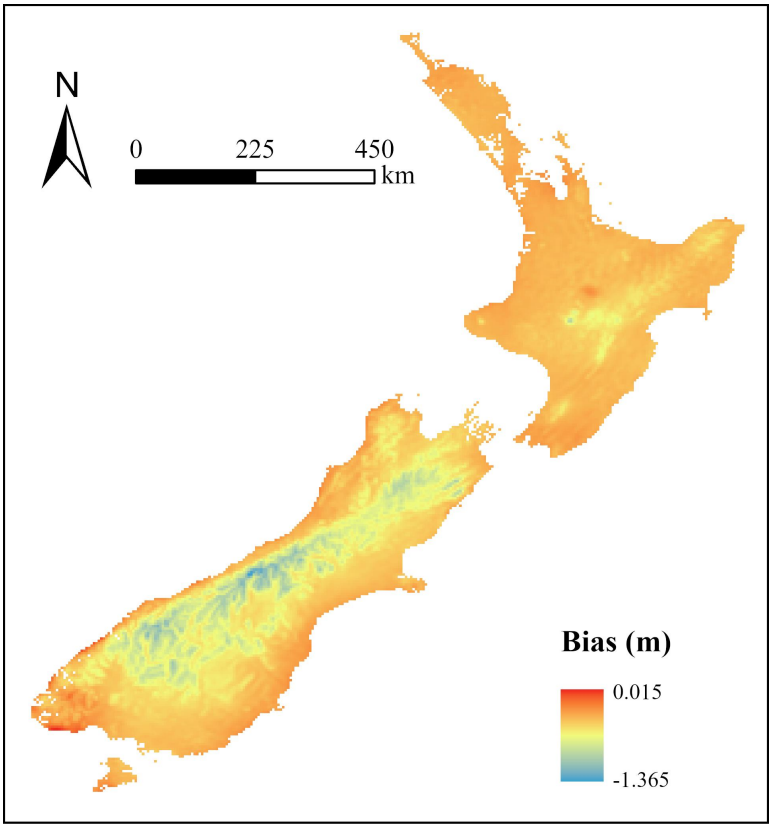

Fig. 1 Spatial distribution of the offset ($N_{EGM2008}-N$) between EGM2008 and NZGeoid2016 across New Zealand. The offset ranges from -1.365 m to 0.015 m. Coastal beach areas show offsets close to zero.

Modifications in the revised manuscript (Section 3.1.1, added after the datum transformation description):

To quantify the spatial variation of the offset between NZVD2016 and EGM2008, we computed the difference between the EGM2008 geoid height and the NZGeoid2016 quasigeoid height ($N_{EGM2008}-N$) on a common grid. The resulting spatial pattern is shown in Fig. S2. The offset ranges from -1.365 m to 0.015 m across New Zealand. Large negative offsets (down to -1.365 m) occur in the South Island mountainous regions, while coastal and beach areas exhibit offsets consistently close to zero (up to 0.015 m).